Computational and structural studies on the complexation of cobalt(II) acetate by water and pyridine

ARTICLE *in* JOURNAL OF MOLECULAR STRUCTURE · JANUARY 2012

Impact Factor: 1.6 · DOI: 10.1016/j.molstruc.2011.09.050

4 AUTHORS, INCLUDING:

Henning Henschel
University of Helsinki
21 PUBLICATIONS **327** CITATIONS
SEE PROFILE

Ian A Nicholls
Linnaeus University
146 PUBLICATIONS **4,257** CITATIONS
SEE PROFILE

Marc Heinrich Prosenc
University of Hamburg
75 PUBLICATIONS **1,260** CITATIONS
SEE PROFILE

Journal of Molecular Structure 1007 (2012) 45–51

Contents lists available at SciVerse ScienceDirect

Journal of Molecular Structure

journal homepage: www.elsevier.com/locate/molstruc

Computational and structural studies on the complexation of cobalt(II) acetate by water and pyridine

Henning Henschel [a], Jan-Peter Klöckner [b], Ian A. Nicholls [a,c], Marc H. Prosenc [b,*]

[a] Bioorganic & Biophysical Chemistry Laboratory, School of Natural Sciences, Linnæus University, 391 82 Kalmar, Sweden
[b] Institute for Inorganic and Applied Chemistry, Department of Chemistry, University of Hamburg, 20 146 Hamburg, Germany
[c] Department of Biochemistry & Organic Chemistry, Uppsala University, 751 23 Uppsala, Sweden

ARTICLE INFO

Article history:
Received 15 April 2011
Received in revised form 26 September 2011
Accepted 26 September 2011
Available online 8 October 2011

Keywords:
Cobalt
Coordination
Crystal structure
Density functional calculation

ABSTRACT

Four different complexes of the cobalt(II) acetate–pyridine–water system were obtained as dominant species by crystallization from a series of dichloromethane and toluene solutions. The complexes were characterized by terms of X-ray crystal structure determination. Factors in solution properties leading to crystallization of certain complexes are discussed. Furthermore, trends in terms of structure and binding energies in a systematic series of mononuclear cobalt(II) complexes were studied using density functional calculations.

1. Introduction

The coordination chemistry of cobalt has long been the subject of research endeavour [1]. Recently, interest in cobalt complexes has once again risen – particularly in conjunction with the catalysis of water oxidation, or the inverse process of oxygen reduction [2–5]. In this context, especially dinuclear complexes make up important model systems [5]. Oligonuclear cluster complexes of cobalt have also been studied as possible catalysts for the oxidation of organic substrates [6,7].

Another field in which cobalt complexes are of importance is in the catalysis of C–C bond formation reactions such as the aldol reaction [8,9]. In conjunction with our own efforts to develop catalytic cobalt complexes of this type [10], we focussed on the properties of complexes of cobalt(II) with pyridine bases. The factors governing the catalytic activity of these systems is not yet fully understood as, owing (amongst others) to the complex nature of solution equilibria, the structures of the catalytically active cobalt complexes have not been revealed yet.

Although a huge number of complexes, and thereby a wide selection of coordination geometries, of cobalt(II) with simple and common ligands such as water and pyridine have been studied, the trends within this group of compounds have barely been investigated.

We report here the structures of a series of cobalt(II) complexes with varying numbers of aqua and pyridine ligands bound to the metal center. Furthermore, we present a series of DFT calculations investigating the trends in binding energies and structure of the complete series of water/pyridine substituted cobalt(II) complexes.

2. Materials and methods

$Co(OAc)_2{\cdot}4H_2O$ has been purchased (Merck102530, Darmstadt, Germany) and used without further purification if not described otherwise. Dichloromethane was purified by distillation from calcium hydride; toluene by distillation from sodium. After purification, solvents were stored under inert conditions. (1*R*)-Benzoylcamphor has been prepared as described [10]. IR spectra were recorded as KBr pellets at a resolution of 2 cm^{-1} on a Bruker Tensor-27 Fourier transform spectrometer, running the OPUS 6.5 version of software.

2.1. Crystallisation of the complexes

2.1.1. Diacetato-tetraaqua-cobalt(II) (**1**)

A solution of $Co(OAc)_2{\cdot}4H_2O$ (69 mg, 0.39 mmol), (1*R*)-benzoylcamphor (100 mg, 0.39 mmol), and pyridine (63 μL, 0.78 mmol) in 1 mL of dichloromethane was prepared. The solvent was allowed to slowly evaporate at room temperature, yielding orange crystals of **1**.

* Corresponding author. Tel.: +49 40 42 838 3102; fax: +49 40 442 838 6945.
E-mail address: prosenc@chemie.uni-hamburg.de (M.H. Prosenc).

0022-2860/$ - see front matter © 2011 Elsevier B.V. All rights reserved.
doi:10.1016/j.molstruc.2011.09.050

*2.1.2. Tetraaqua-dipyridine-cobalt(II) acetate (**2**)*

In 1 mL dichloromethane, $Co(OAc)_2{\cdot}4H_2O$ (69 mg, 0.39 mmol), (1*R*)-benzoylcamphor (100 mg, 0.39 mmol) and pyridine (126 μL, 1.56 mmol) were dissolved. Slow evaporation of the solvent at room temperature gave orange crystals of **2**.

*2.1.3. Diacetato-diaqua-dipyridine-cobalt(II) (**3**)*

$Co(OAc)_2{\cdot}4H_2O$ (69 mg, 0.39 mmol), (1*R*)-benzoylcamphor (100 mg, 0.39 mmol) and pyridine (63 μL, 0.78 mmol) were dissolved under heating in 1 mL of toluene. Crystals of **3** were grown by slow evaporation of the solvent at room temperature. IR: $\tilde{\nu}$ (cm^{-1}) 3110, 3078, 2896, 1603, 1487, 1450, 1361, 1343, 1219, 1156, 1073, 1039, 1025, 1011, 987, 888, 857, 759, 697, 659, 628, 504, 427. Anal. calc. for $C_{14}H_{20}CoN_2O_6$: C, 45.29%; H, 5.43%; N, 7.55%. Found: C, 45.3%; H, 5.41%; N, 7.57%.

*2.1.4. Tetraacetato-tripyridine-dicobalt(II) (**4**)*

$Co(OAc)_2{\cdot}4H_2O$ (429 mg, 1.72 mmol) was dehydrated by cautiously heating under vacuum, keeping the temperature well below 200 °C in order to avoid decomposition of the acetate (which is known to take place around 230 °C [11]), until weight loss corresponding to the four aqua ligands was reached. The resulting violet powder was, together with pyridine (0.54 mL, 6.7 mmol) dissolved in 4.3 mL of toluene under heating to the boiling point. From this solution **4** crystallized over a period of several weeks at 4 °C. IR: $\tilde{\nu}$ (cm^{-1}) 3066, 3003, 2931, 1635, 1619, 1601, 1571, 1486, 1447, 1416, 1339, 1218, 1153, 1075, 1038, 1010, 907, 765, 758, 701, 653, 628, 615, 520, 492, 427. Anal. calc. for $C_{51}H_{59}Co_4N_7O_{16}$: C, 48.55%; H, 4.71%; N, 7.77%. Found: C, 47.1%; H, 4.96%; N, 7.5%.[1]

Crystallisation of **1**–**3** was essentially quantitative. Crystallisation of **4**, however, was accompanied by precipitation of an inhomogeneous, mostly pink, powder, prohibiting exact specification of the yield – it is estimated to approximately 50%.

2.2. Crystal structure determination

Single crystal X-ray diffraction data were collected using a Bruker D8 three circle diffractometer with Smart Apex CCD detector, Oxford Cryostream low temperature device and fine focus Mo Kα sealed tube with graphite monochromator.

180° ω-scans for a total of 2400 frames (0.3°-scan correlated) per measurement with four different ϕ positions ($\Delta\phi = 90°$) were collected. Data reduction and empirical absorption correction were carried out with the program packages SAINT and SADABS [12].

Solution of phase problem and structure refinement were performed with SHELXS and SHELXL, Graphics are from SHELXP [13].

2.3. Electronic structure calculations

All calculations were performed using the Gaussian09 [14] program package. In all cases the B3LYP [15] functional with a LanL2TZ (f) [16–20] basis set for cobalt and a 6-311+G(d,p) [21,22] basis set for all other atoms was used. All cobalt(II) complexes were assumed to exist in high-spin configuration. Geometry optimizations were conducted using the default convergence criteria implemented in the program. Optimized geometries were confirmed to represent energetic minima by frequency calculations yielding only real frequencies.

[1] The elemental composition was calculated assuming exactly 0.5 pyridine molecules per complex molecule, corresponding to maximum occupation of the pyridine site found in the crystal structure. This, however, can, due to the strong disordering of the pyridine, not be fully established from the crystal structure. The deviation of the found composition from the calculated values can be explained by incomplete occupation of this site.

Interaction energies were calculated as difference between the electronic energy of the complex with the ligand in a bound state and the energies of the relaxed structures of the isolated ligand and remaining complex fragment.

3. Results and discussion

We have previously reported efforts to develop molecularly imprinted polymers [23] with class-II aldolase-like activity [10]. The use of analogs of transition states (or reaction intermediates) – (1*R*)-benzoylcamphor in the present case – as templates in the polymer synthesis is intended to yield recognition sites capable of facilitating the conversion of substrates to aldol products. While spectroscopic studies by us [10] and others [24] point toward a direct coordination of the template cobalt center, the nature of the embedded complexes remains elusive.

In order to evaluate the structures of different cobalt(II) complexes, we prepared a series of solutions of cobalt(II) acetate (mostly the tetrahydrate was used) in different solvents, containing between 0 and 6 equivalents of pyridine and generally one equivalent of (1*R*)-benzoylcamphor. Slow evaporation of the solvent from these solutions resulted in the formation of crystalline material that could be investigated by single crystal structure determination (see Table 1).

Although our spectroscopic investigations [10] suggested otherwise analysis of compounds **1**–**3** revealed, that the (1*R*)-benzoylcamphor was not incorporated into the structures, rather already reported structures [25–27] were obtained as crystalline material. Compound **1** has been reported twice according to CCDC database entries COAQAC (RT, R1 = 14%) [28] and COAQAC1 (153 K, R1 = 1.8%) [25]; we reinvestigated the structure at 100 K resulting in a very low *R*-factor of just 1.46% up to $2\theta = 60°$. While our structure of compound **2** is comparable to reported data, complex **3** has previously been investigated at higher temperature and different experimental setup resulting in an inferior *R*-factor compared to our structure. Geometric parameters for compounds **1**–**3** are summarized in Table 2.

Complex **1** crystallizes from a dichloromethane solution of cobalt acetate tetrahydrate with (1*R*)-benzoylcamphor and up to two equivalents of pyridine. While solution spectroscopy experiments indicate a coordination of the (1*R*)-benzoylcamphor, it was not incorporated in the solid state. The complex **1** crystallizes in the monoclinic space group $P2_1/c$ with two molecules per unit cell. The cobalt atom is located on a center of inversion. Two acetato ligands are bound *trans* to each other and four water molecules are bound in a planar arrangement (Fig. 1) completing a sixfold coordination environment. Short distances of Co–O1 of 208.84 pm, and Co–O3 of 208.82 pm and a longer distance Co–O4 of 211.73 pm, and angles of O–Co–O of close to 90° are indicative of an axial distortion of the coordination geometry, resulting in a distorted octahedron with two axial water molecules and two water and two acetato ligands in the equatorial plane. The difference in Co–O distances of the coordinated water molecules O3, O4 and their symmetry equivalents are attributed to the hydrogen bonds between O3 (donor) and O2 (acceptor, see below). The water ligand O4, involved in an intermolecular hydrogen bond to an acetate ligand, exhibits the longest Co–O distance.

Upon increase of the pyridine concentration the two acetato ligands were substituted by two pyridine ligands (complex **2**, Fig. 2). The two acetato ligands remain in the outer sphere coordination environment of the complex [26]. The pyridine ligands are coordinated trans to each other (Co–N1 = 215.53 pm, Co–N2 = 215.15 pm), thus it appears that no coordinative rearrangement can be observed upon substitution of the two acetato ligands. This surprises, as the water ligands, due to their π-donor

Table 1
Crystallographic data for the complexes.

Compound	1	2	3	4
Empirical formula	$C_4H_{14}CoO_8$	$C_{14}H_{24}CoN_2O_8$	$C_{14}H_{20}CoN_2O_6$	$C_{26}H_{30}Co_2N_3O_8$
Formula weight	249.08	407.28	371.25	630.39
Temperature (K)	100(2)	153(2)	100(2)	153(2)
Radiation	Mo Kα			
Wavelength (pm)	71.073			
Diffractometer	D8, IμS (Mo)			
Detector	Smart APEX CCD			
Cell setting	Monoclinic	Monoclinic	Orthorhombic	Monoclinic
Space group	$P2_1/c$ (#14)	$P2_1/m$ (#11)	$Pbca$ (#61)	$P2_1/c$ (#14)
a, b, c (pm)	477.71(1)	835.53(6)	1230.30(02)	899.88(11)
	1184.93(2)	959.05(6)	884.82(2)	1807.2(2)
	827.98(1)	1164.73(8)	1490.75(3)	1777.5(2)
β (°)	92.925(1)	104.989(1)	90	96.657(2)
Volume (nm^3), Z	0.468070(14), 2	0.90156(11), 2	1.62282(6), 4	2.8713(6), 4
Density (calculated) (Mg/m^3)	1.780	1.500	1.520	1.458
Absorption coefficient (mm^{-1})	1.861	0.995	1.089	1.206
F(000)	258	426	772	1300
Crystal size (mm^3)	0.30 × 0.30 × 0.30	0.30 × 0.30 × 0.30	0.54 × 0.53 × 0.52	0.34 × 0.29 × 0.07
Crystal description	Rhombohedron	Rhombohedron	Rhombohedron	Plate
Color	Pink	Pink	Pink	Violet
θ-Range for data collection (°)	3.44–29.98	2.52–27.99	3.15–32.00	2.25–27.50
Index ranges	$-6 \leqslant h \leqslant 6$	$-11 \leqslant h \leqslant 10$	$-17 \leqslant h \leqslant 17$	$-11 \leqslant h \leqslant 11$
	$-16 \leqslant k \leqslant 16$	$-12 \leqslant k \leqslant 12$	$-11 \leqslant k \leqslant 13$	$-23 \leqslant k \leqslant 23$
	$-11 \leqslant l \leqslant 11$	$-15 \leqslant l \leqslant 15$	$-18 \leqslant l \leqslant 22$	$-23 \leqslant l \leqslant 23$
Reflections collected	11,896	10,888	46,059	33,670
Independent reflections	1354	2230	2769	6561
	[R (int) = 0.0155]	[R (int) = 0.0748]	[R (int) = 0.0178]	[R (int) = 0.0699]
Completeness to θ	29.99°, 99.5%	27.99°, 96.7%	32.00°, 98.4%	27.50°, 99.4%
Data/restraints/param.	1354/0/89	2230/0/127	2769/4/113	6561/0/356
Goodness of fit on F^2	1.102	1.075	1.106	0.920
Final R indices [$I > 2\sigma(I)$]	$R1$ = 0.0146	$R1$ = 0.0356	$R1$ = 0.0221	$R1$ = 0.0387
	w$R2$ = 0.0381	w$R2$ = 0.0961	w$R2$ = 0.0628	w$R2$ = 0.0891
R indices [all data]	$R1$ = 0.0150	$R1$ = 0.0377	$R1$ = 0.0241	$R1$ = 0.0610
	w$R2$ = 0.0384	w$R2$ = 0.0975	w$R2$ = 0.0647	w$R2$ = 0.0945
High. peak & deap. hole	0.489; −0.177	1.217; −0.323	0.467; −0.237	0.690; −0.521

Table 2
Selected distances (pm) and angles (°) found in structures of **1**, **2**, and **3**.

Structure	1	2	3
Co–O1	209.84(6)		206.93(6)
Co–O3	208.82(6)	208.71(9)	211.87(6)
Co–O4	211.73(6)	208.87(9)	
Co–N1		215.53(15)	218.02(7)
Co–N2		215.05(16)	
O1–Co–O3	89.51(2)		89.91(2)
O1–Co–O4	89.68(2)		
O3–Co–O4	89.43(2)	89.89(4)	
O1–Co–N1			89.96(3)
O3–Co–N1		86.65(4)	89.20(3)
O4–Co–N1		93.52(4)	
N1–Co–N2		179.77(4)	

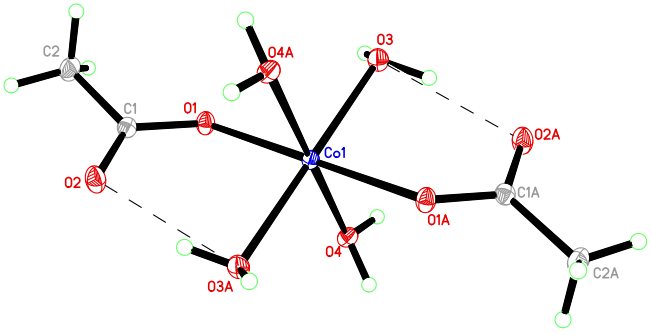

Fig. 1. Diagram of **1**, showing 50% thermal ellipsoid probability. Symmetry operation to display the indexed atoms: $-x$, $1-y$, $1-z$.

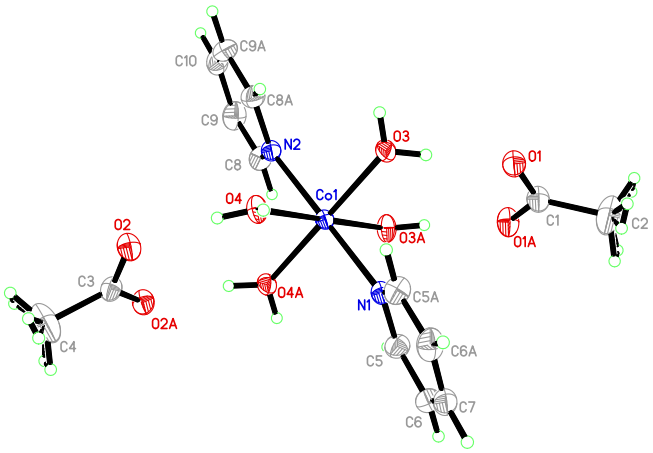

Fig. 2. Diagram of **2**, showing 50% thermal ellipsoid probability. Symmetry operation to display the indexed atoms: x, $0.5-y$, z.

capabilities, are expected to significantly destabilize the t_{2g} orbitals at the cobalt center. This is unexpected for the acetato ligands. The bond to the pyridine ligand is found to deviate slightly from the plane of the pyridine ring, reducing nonbonding repulsions or alternatively due to induced dipolar interactions. Short distances of Co–O3 of 208.71 pm and Co–O4 of 208.87 pm in conjunction with intermolecular hydrogen bond distances to the two actetato ions are comparable with the distances found in complex **1** for the hydrogen bonded water ligands. Angles around the cobalt center deviate less than 4° from octahedral symmetry.

If a solvent with lower polarity was used, i.e. toluene, the acetato ligands remain bound to the cobalt(II) center. Crystallization from a mixture containing **1** together with a minimum of two equivalents of pyridine in toluene by slow evaporation resulted in formation of crystals of complex **3**. In complex **3** two of the aqua ligands were substituted by the pyridine molecules, which bind with a *trans* relationship to each other (see Fig. 3). The Co–O3 bond in complex **3** of 211.9 pm was found to be the longest water to cobalt bond in the series of investigated complexes. An intramolecular hydrogen bond was found between O2 (acceptor) and O3 (donor) of 269.2 pm. In contrast, a bond Co to O1 of 206.93 pm was found to be the shortest within the series. Angles O–Co–N and O–Co–O of close to 90° are indicative of a nearly octahedral coordination environment around the Co-center.

All three complexes exhibit a pseudo octahedral coordination geometry with only small deviations in angles from 90°. The distances between the water molecules and the metal center deviate but reveal no conclusive trend for the bond lengths. Intramolecular hydrogen bonding interaction appears to be the cause for the shortening in complexes **1** and **2**. In complex **3**, however, despite a similar hydrogen bridge, the longest Co–O bond was found. In order to be able to differentiate between intra- and intermolecular interactions electronic structure calculations were performed with emphasis on the Co(II) water ligand bond strength. As these are performed on the isolated molecules, they in particular allow to determine whether non-bonding repulsions or electronic distortion are the cause of the bond length alternation (see below).

Even from reaction mixtures containing six equivalents of pyridine, no crystalline material could be obtained in which all aqua ligands were substituted. A complex without aqua ligands could only be obtained when the reaction mixture was kept completely free of water. Even in that case, however, no more than two pyridine ligands were found to coordinate to one cobalt center under the conditions studied, leading to the formation of the dinuclear complex **4**. By the inverse route of 2,2′-bipyridine addition to a polymeric cobalt(II) system, a series of related dinuclear cobalt(II) complexes have earlier been obtained [29,30].

Structure **4** (see Table 3 for a summary of geometric parameters) exhibits a coordination environment that has not been observed before for cobalt, with two bridging acetato ligands, one acetato ligand bound dihapto to each cobalt center, one of which also bridges with one oxygen atom to the other cobalt atom. Hexacoordination of both cobalt atoms is completed by one and

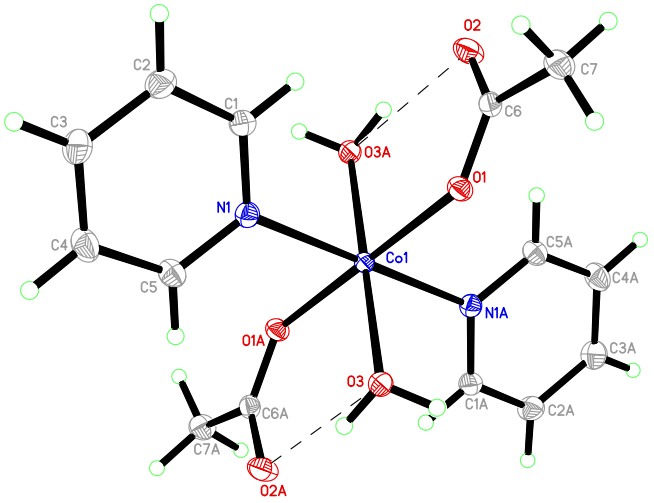

Fig. 3. Diagram of **3**, showing 50% thermal ellipsoid probability. Symmetry operation to display the indexed atoms: 1 − *x*, −*y*, 1 − *z*.

Table 3
Selected distances (pm) and angles (°) found in structure **4**.

Structure	**4**
Co1–Co2	346.69(5)
Co1–O2	203.36(18)
Co1–O3	210.86(18)
Co1–O4	222.38(19)
Co1–O6	204.44(18)
Co1–O8	214.89(18)
Co1–N1	214.2(2)
Co2–O1	206.19(18)
Co2–O5	202.41(18)
Co2–O7	217.05(18)
Co2–O8	216.90(17)
Co2–N2	219.2(2)
Co2–N3	211.7(2)
Co1–O8–Co2	106.82(7)
O1–Co2–O5	95.26(8)
O1–Co2–O7	90.35(7)
O1–Co2–O8	93.49(7)
O1–Co2–N3	85.49(7)
O2–Co1–O3	159.31(7)
O2–Co1–O4	98.70(7)
O2–Co1–O6	105.40(7)
O2–Co1–O8	88.77(7)
O2–Co1–N1	87.89(8)
O3–Co1–O8	91.51(7)
O3–Co1–N1	92.49(8)
O5–Co2–N2	88.42(8)
O5–Co2–N3	95.99(8)
N2–Co2–N3	88.64(8)

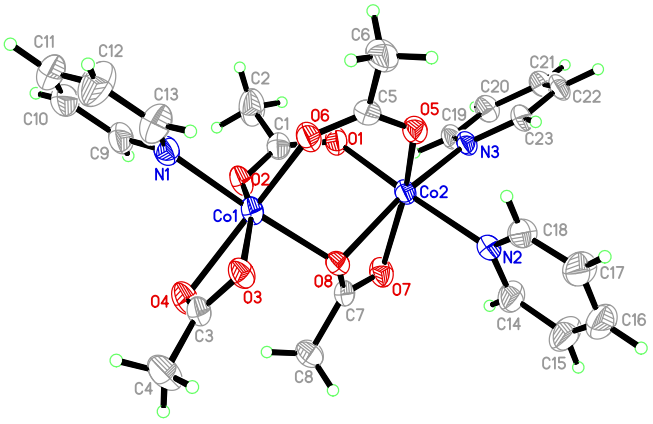

Fig. 4. Diagram of **4**, showing 50% thermal ellipsoid probability. The co-crystallized pyridine molecule was omitted for clarity.

two pyridine ligands, respectively (Fig. 4). The asymmetric unit also contains half a molecule of pyridine. Due to the fact that the pyridine molecule lies on the center of inversion and no favorable orientation could be established based on donor aceptor interactions, the best model for refinement of the highly disordered solvent molecule was found to be as half a molecule of benzene. Residual density peaks implying diffuse disorder were neglected.

The two cobalt atoms in structure **4** are separated by a non-bonded distance of 346.7 pm. The non-bridging acetato ligand is bound with two considerably different Co–O distances to Co1 (210.9 and 222.4 pm, respectively), while the bridging dihapto acetato ligand exhibits comparable distances for all three Co–O bonds (d(Co1–O8) = 214.9 pm, d(Co2–O7/8) = 217.1; 216.9 pm). This is in clear contrast to the situation in the crystal structure of a previously described (nickel) complex with an identical immediate coordination environment, in which a non-bridging carboxylato ligand binds symmetrically, while the bridging dihapto ligand

exhibits different Co–O bond distances [31]. The bond distances between the dihapto acetato oxygen atoms and cobalt center in structure **4** are considerably longer than those found in the mononuclear complexes **1**–**3**, which can be attributed to the strained binding mode of the acetato ligands (α(O–Co–O) = 60.7°). This relatively weak binding is balanced by bond distances to ligands in *trans*-position relative to these oxygen atoms being substantially contracted (202 pm $\leqslant$ *d*(Co–O) $\leqslant$ 204 pm; *d*(Co2–N3) = 211.7 pm). For the Co1–N1 bond that is in *trans*-position relative to the bridging oxygen atom O8, this effect is less pronounced – its length is with 214.2 pm only slightly shorter than the Co–N distances observed in structures **2** and **3**. Compared to the distance between Co2 and N2 that stands *trans* to the Co2–O1 bond (which with 206.2 pm has a length comparable to those in structures **1** and **3**) of 219.2 pm, however, the difference is significant.

Structure **4** illustrates quite clearly the effect the considerable spatial requirements of pyridine as a ligand in complexes with small metal ions as cobalt(II) have. Rather than a third pyridine ligand binding to any one cobalt center, the acetato ligands bind with both oxygen atoms, bridging two cobalt centers, or bind as dihapto ligands.

The structural element of acetato ligands acting as dihapto ligands is also observed in the structures resulting from the calculations performed (Fig. 5) in cases where the cobalt center would otherwise be coordinatively unsaturated. It is, however, only observed if the second oxygen atom of the acetato ligand is not involved into an intramolecular hydrogen bond with an aqua ligand.

Another noteworthy feature found in the calculated structures is the distinct deviation in the orientation of the aqua ligands in **aq_4** compared to the corresponding crystal structure (**1**). In this crystal structure two sets of two water molecules with different bond conformations can be found, while in the calculated structure **aq_4** all four water molecules are oriented differently. The symmetric arrangement of the aqua ligands in the crystalline system makes it possible to build up an extended hydrogen bond network as already has been described for this structure by Sobolev et al. [25]. In the calculation of the isolated complex, however, the non-spherical distribution of the d-electrons can lead to slight differences in the coordination of the aqua ligands, which – in conjunction with the geometric requirements for formation of hydrogen bonds with the acetato ligands – can lead to the observed dissymmetry.

Table 4
Cobalt–oxygen and cobalt–nitrogen distances in the calculated hexacoordinated complexes.

Structure	aq_4	aq_3py_1	*cis*-aq_2py_2	*trans*-aq_2py_2	aq_1py_3	py_4
d (Co–O_{aq}) (pm)	211.8	213.3	220.3	215.6	217.6	
	216.6	219.2	220.5	215.6		
	218.7	223.8				
	222.0					
d (Co–O_{ac}) (pm)	202.4	207.9	209.9	209.9	206.8	209.1
	210.8	208.5	210.1	209.9	213.3	209.1
d (Co–N) (pm)		214.4	219.1	220.1	222.4	223.1
			219.1	220.1	222.7	223.2
					223.4	223.2
						223.4

As evident from the data compiled in Table 4, the calculations generally yield larger Co–O_{aq} distances than those observed in the crystal structures. The strong influence of hydrogen bonds on the length of bonds between cobalt and aqua ligands that was observed in the crystal structures, however, is also observed for the calculated structures. Even though the calculated systems are confined to intramolecular hydrogen bonds, still they have enough impact to – similar to the situation in the crystal structures – obscure any possible clear trends in Co–O bond lengths. The Co–N distances obtained from calculations are systematically larger than those from the crystal structures. Here, however, a clear, though small, trend toward longer bond lengths with increasing number of pyridine ligands can be seen. While this can be expected to be mainly due to steric crowding, the comparison between the *cis*- and *trans*-isomer of the diaqua dipyridine complex suggests that the stronger *trans* effect of pyridine as compared to water might also be of importance [32].

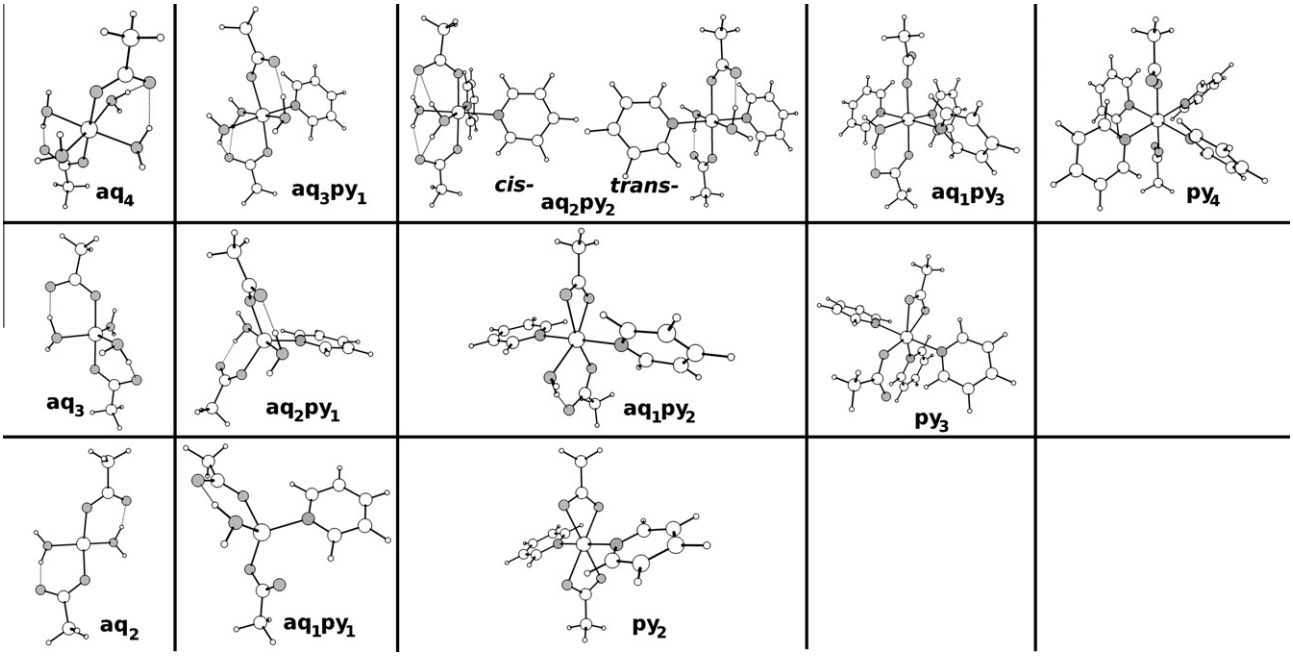

Fig. 5. Series of calculated structures. Downward movement (↓) corresponds to loss of one water ligand, rightward movement (→) corresponds to substitution of one water by one pyridine ligand.

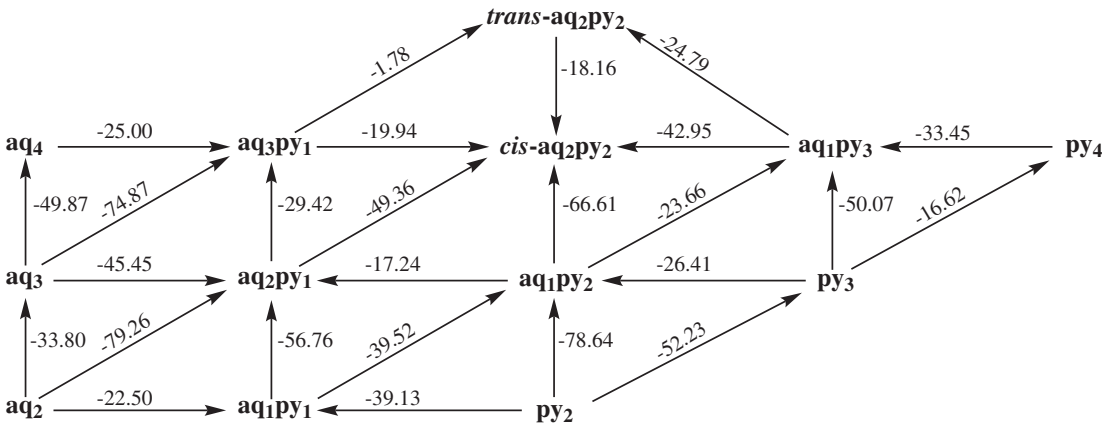

Fig. 6. Energies of the transformations between the different calculated complexes in kJ/mol. Direction of arrows is chosen to always represent exergonic processes.

Calculations of the energies for a series of structures corresponding to the crystal structures resulted in the *cis*-diaqua-dipyridine complex being the most stable within the series. As visualized in Fig. 6, two main trends can be observed in the relative energies that lead to this fact. Binding energies of the first two water molecules to the metal center are significantly higher than those of the third and fourth. This can be explained by the strong hydrogen bonds between the first two aqua and acetato ligands that can be observed in the structures. The formation of additional hydrogen bonds with the third and fourth aqua ligand simultaneously weakens the binding interaction with the other two aqua ligands. Another trend, which can be observed is that the binding of a third or fourth pyridine ligand to form a hexacoordinated complex yields much less energy than the binding of a pyridine ligand in all other situations. One important factor for this can be expected to be steric crowding.

In the comparison between the two configurations of the di-aqua-dipyridine cobalt(II) it can be seen that in the *cis*-configuration both hydrogen atoms of both aqua ligands are involved in hydrogen bonds with the acetato ligands, while in the *trans*-configuration one hydrogen atom of each water molecule is not bound ("dangling"). In the crystal structure (or in a polar solvent) the energy difference between the two configurations can be expected to be shifted in favor of the *trans*-configurations as these dangling hydrogen atoms can become involved into hydrogen bonds with the acetato ligands of neighboring complex (or solvent) molecules. Another factor leading to the observation of the *trans*-complex instead of the *cis*-complex the crystal structure might be the larger *trans*-effect of the pyridine ligand as compared to the aqua ligand.[2]

In a similar fashion the general trend toward more aqua ligands than would be expected from the calculations as observed in the crystal structure can be explained by the formation of hydrogen bonds with neighboring complex molecules that are not covered in the calculations.

4. Conclusions

We were able to present the structures of a conclusive series of cobalt(II) complexes with different numbers of aqua, pyridine, and acetato ligands, together with the conditions under which they crystallize. One of the structures obtained (**4**) represents a structure of a dinuclear complex with a for cobalt hitherto unknown coordination environment with three different binding modes of the acetato ligands.

Results showed that if water is present, it binds to the cobalt center. This is consistent with the results from the calculations showing a net energy penalty for substitution of the third and fourth aqua ligand by pyridine, i.e. the diaqua-dipyridine complexes (*trans*- and *cis*-$\mathbf{aq_2py_2}$) were found to be most stable. The additional difficulty to substitute the first aqua ligands observed in the crystallization experiments is likely originated from the stabilizing effect of intermolecular hydrogen bonds – especially in solid state. The opposite of this effect seems to be the case for the (1*R*)-benzoylcamphor used in the experiments leading to structure **1**–**3** – even though spectroscopic evidence exists for it acting as a ligand, it is not found to be incorporated into the crystal phase.

Furthermore, the possibility of coordination of more than two pyridine ligands to form a hexacoordinated complex is considered unlikely, both from experimental as well as calculated results.

Acknowledgments

We thank Thorsten Werner for generous support with computations. For funding the Deutsche Forschungsgemeinschaft (Grant Nos. DFG-SPP1178/P-654/3 and DFG-SFB668/A4), and the Swedish Research Council (2006-6041) are gratefully acknowledged.

Appendix A. Supplementary material

Supplementary data associated with this article can be found, in the online version, at doi:10.1016/j.molstruc.2011.09.050.

References

[1] A. Werner, Ber. Dtsch. Chem. Ges. 44 (1911) 1887–1898.
[2] H. Dau, C. Limberg, T. Reier, M. Risch, S. Roggan, P. Strasser, ChemCatChem 2 (2010) 724–761.
[3] T.R. Cook, D.K. Dogutan, S.Y. Reece, Y. Surendranath, T.S. Teets, D.G. Nocera, Chem. Rev. 110 (2010) 6474–6502.
[4] Q. Yin, J.M. Tan, C. Besson, Y.V. Geletii, D.G. Musaev, A.E. Kuznetsov, Z. Luo, K.I. Hardcastle, C.L. Hill, Science 328 (2010) 342–345.
[5] M. Volpe, H. Hartnett, J.W. Leeland, K. Wills, M. Ogunshun, B.J. Duncombe, C. Wilson, A.J. Blake, J. McMaster, J.B. Love, Inorg. Chem. 48 (2009) 5195–5207.
[6] R. Chakrabarty, D. Kalita, B.K. Das, Polyhedron 26 (2007) 1239–1244.
[7] C.E. Sumner, G.R. Steinmetz, J. Am. Chem. Soc. 107 (1985) 6124–6126.
[8] J. Park, K. Lang, K.A. Abboud, S. Hong, J. Am. Chem. Soc. 130 (2008) 16484–16485.
[9] Z. Chen, M. Furutachi, Y. Kato, S. Matsunaga, M. Shibasaki, Angew. Chem. Int. Ed. 48 (2009) 2218–2220.
[10] J. Hedin-Dahlström, J.P. Rosengren-Holmberg, S. Legrand, S. Wikman, I.A. Nicholls, J. Org. Chem. 71 (2006) 4845–4853.
[11] R.W. Grimes, A.N. Fitch, J. Mater. Chem. 1 (1991) 461–468.

[2] Optimization of complex **3** in low spin state revealed longer axial Co–O_{aq} bonds and shorter equatorial Co–$O_{acetate}$ and Co–N bonds which points toward a possible mixture of high and low spin states in solid state at 153 K.

[12] Apex2 (version 2.1), saint (version 7.34a), sadabs (version 2.03) and xprep (version 2005/4), 2006. Bruker AXS Inc., Madison, Wisconsin, USA.
[13] G.M. Sheldrick, Acta Crystallogr. A 64 (2007) 112–122.
[14] M.J. Frisch, G.W. Trucks, H.B. Schlegel, G.E. Scuseria, M.A. Robb, J.R. Cheeseman, G. Scalmani, V. Barone, B. Mennucci, G.A. Petersson, H. Nakatsuji, M. Caricato, X. Li, H.P. Hratchian, A.F. Izmaylov, J. Bloino, G. Zheng, J.L. Sonnenberg, M. Hada, M. Ehara, K. Toyota, R. Fukuda, J. Hasegawa, M. Ishida, T. Nakajima, Y. Honda, O. Kitao, H. Nakai, T. Vreven, J.A. Montgomery Jr., J.E. Peralta, F. Ogliaro, M. Bearpark, J.J. Heyd, E. Brothers, K.N. Kudin, V.N. Staroverov, R. Kobayashi, J. Normand, K. Raghavachari, A. Rendell, J.C. Burant, S.S. Iyengar, J. Tomasi, M. Cossi, N. Rega, J.M. Millam, M. Klene, J.E. Knox, J.B. Cross, V. Bakken, C. Adamo, J. Jaramillo, R. Gomperts, R.E. Stratmann, O. Yazyev, A.J. Austin, R. Cammi, C. Pomelli, J.W. Ochterski, R.L. Martin, K. Morokuma, V.G. Zakrzewski, G.A. Voth, P. Salvador, J.J. Dannenberg, S. Dapprich, A.D. Daniels, Ö. Farkas, J.B. Foresman, J.V. Ortiz, J. Cioslowski, D.J. Fox, Gaussian 09 Revision A02, Gaussian Inc., Wallingford, CT, 2009.
[15] A.D. Becke, J. Chem. Phys. 98 (1993) 5648–5652.
[16] P.J. Hay, W.R. Wadt, J. Chem. Phys. 82 (1985) 270–283.
[17] P.J. Hay, W.R. Wadt, J. Chem. Phys. 82 (1985) 299–310.
[18] W.R. Wadt, P.J. Hay, J. Chem. Phys. 82 (1985) 284–298.
[19] L.E. Roy, P.J. Hay, R.L. Martin, J. Chem. Theory Comput. 4 (2008) 1029–1031.
[20] A. Ehlers, M. Böhme, S. Dapprich, A. Gobbi, A. Höllwarth, V. Jonas, K. Köhler, R. Stegmann, A. Veldkamp, G. Frenking, Chem. Phys. Lett. 208 (1993) 111–114.
[21] R. Krishnan, J.S. Binkley, R. Seeger, J.A. Pople, J. Chem. Phys. 72 (1980) 650–654.
[22] T. Clark, J. Chandrasekhar, G.W. Spitznagel, P.V.R. Schleyer, J. Comput. Chem. 4 (1983) 294–301.
[23] C. Alexander, H.S. Andersson, L.I. Andersson, R.J. Ansell, N. Kirsch, I.A. Nicholls, J. O'Mahony, M.J. Whitcombe, J. Mol. Recognit. 19 (2006) 106–180.
[24] C.J. Allender, O.K. Castell, P.R. Davies, S. Fiddy, J. Hedin-Dahlström, M. Stockenhuber, Chem. Commun. (2009) 165–167.
[25] A.N. Sobolev, E.B. Miminoshvili, K.E. Miminoshvili, T.N. Sakvarelidze, Acta Crystallogr., Sect. E: Struct. Rep. Online 59 (2003) m836–m837.
[26] J.K. Clegg, M.J. Hayter, K.A. Jolliffe, L.F. Lindoy, Acta Crystallogr., Sect. E: Struct. Rep. Online 62 (2006) m873–m874.
[27] A. Bailey, W.P. Griffith, D.W. Leung, A.J. White, D.J. Williams, Polyhedron 23 (2004) 2631–2636 (Special Issue in honour of M.L.H. Gree).
[28] J.N. van Niekerk, F.R.L. Schoening, Acta Crystallogr. 6 (1953) 609–612.
[29] M.O. Talismanova, A.A. Sidorov, V.M. Novotortsev, G.G. Aleksandrov, S.E. Nefedov, I.L. Eremenko, I.I. Moiseev, Russ. Chem. Bull. 50 (2001) 2251–2253.
[30] I.G. Fomina, A.A. Sidorov, G.G. Aleksandrov, V.I. Zhilov, V.N. Ikorskii, V.M. Novotortsev, I.L. Eremenko, I.I. Moiseev, Russ. Chem. Bull. 53 (2004) 118–126.
[31] A.A. Sidorov, I.G. Fomina, A.E. Malkov, A.V. Reshetnikov, G.G. Aleksandrov, V.M. Novotortsev, S.E. Nefedov, I.L. Eremenko, Russ. Chem. Bull. 49 (2000) 1887–1890.
[32] M.P. Mitoraj, H. Zhu, A. Michalak, T. Ziegler, Int. J. Quant. Chem. 109 (2009) 3379–3386.